The role of m6A-related lncRNAs on prognosis and chemo radiotherapy response of osteosarcoma: potential molecular pathways

Y. Zhou[3#], Y. Bi[1,2#], M. Wan[1,2], N. Xu[4], Y. Xu[1,2], P. Liu[1,2], H. Jiang[1,2], H.Fang[1,2], H. Hu[1,2], S. Xu[1,2*], S. Lan[1,2*]

[1]*Department of Orthopaedics, Shanghai Eighth People's Hospital, Jiangsu University, Shanghai 200235, China*
[2]*Department of Orthopaedics, Xuhui Branch of Shanghai Sixth People's Hospital Affiliated to Shanghai Jiao Tong University School of Medicine, Shanghai 200233, China*
[3]*Department of Anesthesiology, Dongfang Hospital of Beijing University of Chinese Medicine, Beijing, 100078, China*
[4]*Department of Orthopaedics, Shanghai Sixth People's Hospital Affiliated to Shanghai Jiao Tong University School of Medicine, Shanghai 200233, China*

► *Original article*

# These authors contributed equally to this work.

ABSTRACT

Background: Conventional treatments on osteosarcoma (OS) yield limited improvements in metastatic or relapsed cases, necessitating innovative therapeutic strategies. This study's objective is to reveal the role of long non-coding RNAs (lncRNAs) in prognosis and potential molecular pathways of OS. ***Materials and Methods:*** This study integrated bioinformatics, statistical analysis, and computational techniques to investigate m6A-related prognostic lncRNA clusters in OS. Consensus clustering and risk analysis were performed on the m6A-related prognostic lncRNAs. Nomogram model was built for survival prediction, and was assessed using survival time receiver operator characteristic (ROC) analysis and decision curves. A competitive endogenous RNA (ceRNA) network was built to explore lncRNA-miRNA (microRNA)-mRNA interactions using the microRNA database and metascape website, followed by functional enrichment analyses. ***Results:*** The analysis unveiled three distinct OS clusters, with Cluster 2 exhibiting the highest risk in the immune microenvironment. High risk 7-lncRNA signature demonstrated strong prognostic value in predicting OS overall survival. The ceRNA network highlighted complex interactions among mRNAs, miRNAs and lncRNAs. Functional enrichment analysis indicated that mRNAs within the ceRNA network were linked to many biological functions. Furthermore, 30 differentially expressed genes (DEGs) derived from low-risk and high-risk groups enriched in GO-BP connected to MAGE (melanoma antigen gene) family member A2 (MAGEA2) and MAGEA2B. These DEGs in high risk group were also upregulated in the three KEGG (Kyoto Encyclopedia of Genes and Genomes) pathway. ***Conclusion:*** This study disclosed the role of high-risk m6A-associated lncRNAs in prognosis and potential molecular pathways of OS. These findings provided novel insights into OS pathogenesis and potential therapeutic targets, warranting further validation in clinical settings.

INTRODUCTION

Osteosarcoma (OS) corresponds to around 56% of malignant bone cancers and is the greatest common aggressive bone tumor, mainly affecting pediatric, adolescent, and young adult populations with a median age of 16 years [1, 2]. The current management standards for OS involve extensive surgical resection, neo-adjuvant chemotherapy, and additional chemotherapy [3]. OS is known for its strong tendency toward local aggressiveness and early metastasis, as evidenced by the relapse experienced by 30-50% of patients [4]. About 68% of individuals with locally acquired OS survival for five years or longer [5].

Unfortunately, 20-30% of individuals are diagnosed with metastatic or relapsed cases [6, 7]. Despite the use of certain anticancer agents, the outcomes for both metastatic and relapsed OS have shown little improvement over the past few decades [8]. Given these challenges with traditional therapeutic options, It is imperative that novel therapeutic approaches be developed in order to enhance overall survival rates in OS patients. Moreover, identifying new prognostic markers for OS prognosis is crucial for improving the survival prospects of individuals with OS.

An RNA transcript that is longer than 200 nucleotides is referred to as a long non-coding RNA (lncRNA). Even though they don't usually encode

proteins, lncRNAs play crucial roles in cellular processes such as metabolism, apoptosis, differentiation, proliferation and activation via controlling the expression and function of genes [9]. According to recent studies, dysregulated lncRNAs play essential roles in various disorders, including neoplasms, cardiovascular conditions, and metabolic disorders [10, 11]. Furthermore, dysregulated lncRNAs are strongly linked to patient outcomes in many types of cancer, and were regarded as potential biomarkers and therapeutic targets for diagnosing and managing cancers [12-14]. Also, many abnormal expressions of lncRNAs are intimately connected to the prognosis and therapeutic targets of OS [15-18]. Therefore, lncRNAs can be used as predictable biomarkers to indicate prognosis or promising targets for personalized therapy. Recently, there has been an increase in interest in the m6A and lncRNA study paradigm [19, 20]. Their regulatory complexes are associated with metastasis, migration and tumor growth with different cancers, offering novel targets for cancer diagnosis and treatment [21, 22]. In our recent report, we have revealed that seven m6A-related prognostic lncRNAs (LINC00538, LINC01982, LINC00910, LINC01474, TFPI2-DT, WWC2-AS1 and TNS1-AS1) were associated with OS risk [23], but the potential regulation mechanisms are unclear. Bioinformatics is an emerging field in biological research focused on mathematical, analytical, and computational techniques for the examination and interpretation of biological data. The exponential growth of data from advanced techniques such as microarray technology and genome sequencing has rendered conventional gene-by-gene methods insufficient to address the increasing demands of bioresearch. Consequently, bioinformatics plays a critical role in advancing our comprehension of biology and in the creation of cutting-edge therapeutic approaches. Employing bioinformatics and statistical analysis, In order to increase patient survival rates, we created a risk-based prognosis model to find OS prognostic biomarkers associated with the m6A-related prognostic lncRNAs. This work is new because it takes a fresh approach to treating OS and identifies novel molecular pathways and markers that together advance our knowledge of the disease and possible therapeutic approaches.

MATERIALS AND METHODS

Cluster identification of m6A-related prognostic lncRNAs

Seven m6A-related prognostic lncRNAs associated with OS risk that has been reported in the previous study were identified using univariate Cox analysis long intergenic non-protein coding RNA 538 (LINC00538)) [23], long intergenic non-protein coding RNA 1982 (LINC01982), long intergenic non-protein coding RNA 910 (LINC00910), TFPI2 divergent transcript (TFPI2-DT), WWC2 antisense RNA 1 (WWC2-AS1), (TNS1-antisense RNA 1 (TNS1-AS1). A consistent cluster analysis was performed with the expression profiles of above 7 m6A-related prognostic lncRNAs related to disease risk using Consensus Cluster Plus, and the cluster number was set to 3.

The risk analysis in the immune microenvironment

Using 22 different kinds of immune cells, the cell-type identification by estimating relative subsets of RNA transcripts (CIBERSORT) method was used to determine immune infiltration in patient tissues [24]. The immune cell infiltration scores across samples from Cluster1, Cluster2, and Cluster 3 obtained above were compared using the LM22 feature matrix file and the CIBERSORT method (with 1000 permutations). The results were then shown using box plots. Immune scores, comprising ESTIMATE score, Immune score, Stromal score, and Tumor Purity, were calculated for the TCGA (the cancer genome atlas)-OS expression profiles using the ESTIMATE software. The ggplot2 software was then used to create box plots using samples from Cluster1, Cluster2, and Cluster 3. Additionally, *p*-values among intergroup differences were assessed using the *t*-test.

The predictive nomogram construction

In light of the multi-factor Cox regression analysis's findings, 7 m6A-related prognostic lncRNAs associated with disease risk were identified [23]. The regression coefficients and expression profiles of 7 m6A-related prognostic lncRNAs were then employed to calculate the risk score. The following is the calculating formula: Coef (lncRNAn)×expr (lncRNAn) = risk score. Based on the previously calculated risk scores and survival information (survival time, survival status), a survival model was constructed using the "psm" function from the "rms" package. Subsequently, nomograms were generated using the nomogram function to depict the predicted survival probabilities at 3-year and 5-year time points. The calibrate function from the rms package was employed to calibrate the previously constructed psm model. Calibration was performed at two different time points, namely 5 years (1825 days) and 3 years (1095 days). The resulting calibration curves for both time points were plotted together on a single graph.

The predictive nomogram evaluation

In samples where survival status and survival duration are present, the survival time survival time receiver operator characteristic (ROC) analysis was done through the survival ROC package and plotted as high risk and low risk (or grouped as stage 1/2 and stage 3/4). The risk scores and survival information (survival time, and survival status) were extracted

and decision curves were done using the rmda package. The net benefit curves were plotted using the plot-decision curve function, and the clinical impact curves were plotted using plot-clinical impact. Risk scores were extracted along with survival information (survival time and survival status). The rmda package was utilized to perform decision curve analysis. The functions plot_decision_curve and plot_clinical_impact was employed to generate net benefit curves and clinical impact curves, respectively.

The ceRNA (competitive endogenous RNA) networks

The lncRNA-miRNA (microRNA) reciprocal pairs were obtained from the microRNA database (http://www.mircode.org/download.php), downloading the highly conserved microRNA families' file. Then, we searched for interacting miRNAs with the 7 m6A-related prognostic lncRNAs obtained above in the microRNA dataset, forming lncRNA-miRNA interactional pairs. A total of 147 interactional pairs were obtained. The miRNAs obtained in the previous step were imported into the miR-Walk website (http://mirwalk.umm.uni-heidelberg.de/ search _genes /) to obtain miRNA-mRNA interaction pairs. 421 miRNA-mRNA interaction pairings in total were found. Combining the above lncRNA-miRNA interactions with miRNA-mRNA interactions, lncRNA-miRNA-mRNA interactions were obtained.

The mRNA enrichment analysis of the ceRNA network

Making use of the aforesaid risk scores' median, all OS samples containing survival information were divided into low-risk and high-risk groups. Based on, low-riskand high-risk groups and the gene expression profiles of all genes in OS samples, differential analysis was carried out employing the limma package, setting a threshold of p value < 0.05. A sum of 30 differentially expressed genes (DEGs) were identified in the high-risk versus low-risk comparison.

There was two parts in the enrichment analysis. One part involved 182 mRNA genes within the ceRNA network, and the other part consisted of 30 DEGs obtained from the low-risk and high-risk groups according to the risk score. However, the limited number of DEGs prevents their analysis on the metascape website. Then, 182 mRNAs were extracted from the ceRNA network and imported to the metascape website (https://metascape.org/gp/index.html#/main/step1). KEGG (Kyoto Encyclopedia of Genes and Genomes) pathway enrichment analyses and Gene Ontology (GO) were performed on 30 DEGs using the R language clusterProfiler package (p.adjust < 0.05). The top5 with the most significant GO functional p-values were selected to draw a circle diagram. The pathways enriched by KEGG were

selected and shown in bubble and heat maps, with heat maps grouped as high risk and low risk.

RESULTS

Identification of m6A-related prognostic lncRNAs clusters using univariate Cox analysis

With the R package named Consensus_Cluster_Plus, seven m6A-related prognostic lncRNAs related to OS risk were selected and consistency-cluster analysis was performed. The consensus clustering study indicated that the ideal number of clusters was k = 3 from k = 2 to 9 (figure 1A-C). Three subgroups, designated as Cluster 1, Cluster 2, and Cluster 3, were produced as a consequence of this investigation.
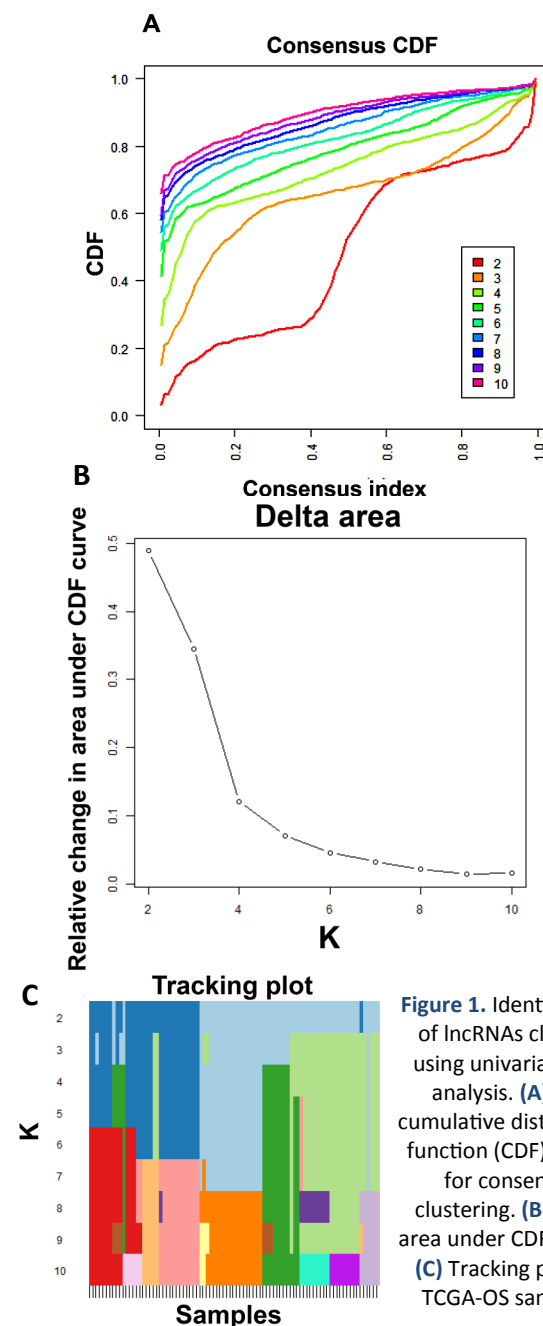

Figure 1. Identification of lncRNAs clusters using univariate Cox analysis. **(A)** The cumulative distribution function (CDF) curves for consensus clustering. **(B)** Delta area under CDF curves. **(C)** Tracking plots in TCGA-OS samples.

The immune microenvironment among the different risk score cluster subgroups

The CIBERSORT algorithm was used to detect immunological infiltrates in the tissues of patients by 22 various subtypes of immune cells. No obvious difference was found in the various subtypes of immune cells, as seen in figure 2A. Furthermore, samples were divided into groups with high and low risk according to the risk ratings determined by patient characteristics. There was none of difference between low-risk and high-risk groups in the four aspects of Tumor Purity, Stromal score, Immune score and ESTIMATE score (figure 2B). The risk core scores were grouped into Cluster 1, Cluster 2 and Cluster 3 in the end. The Cluster2 displayed the highest scores in contrast to Cluster1 ($p<0.05$) and Cluster3 ($p<0.001$), while Cluster3 exhibited the lowest scores among these three clusters (figure 2C, $p<0.001$). These results could imply that the patients with Cluster2 favored high-risk scores compared to those with higher immune Cluster1 and Cluster3 in the OS immune microenvironment.
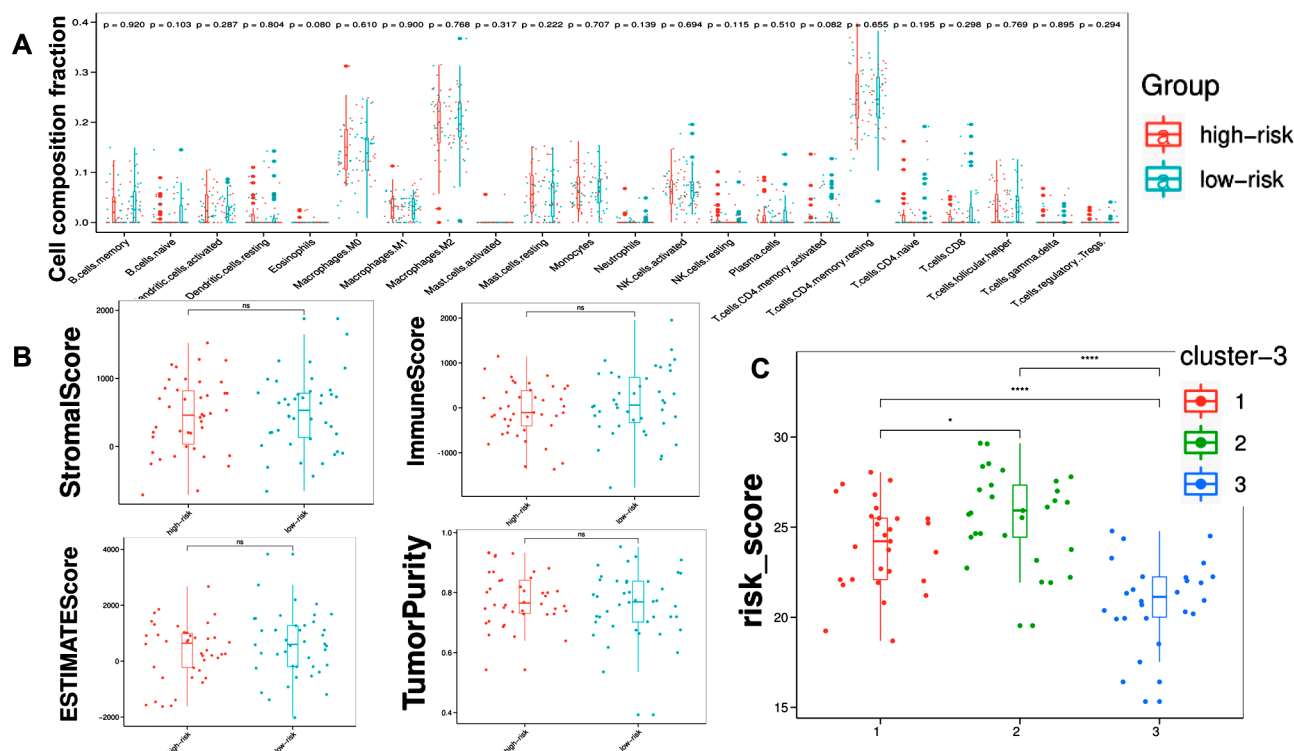

Figure 3. The immune microenvironment among the different risk score cluster subgroups. **(A)** Immunological cell infiltration abundance in OS samples from both low- and high-risk populations. **(B)** The infiltration scores of TumorPurity, ESTIMATEscore, Stromalscore and Immunescore between low- and high-risk groups. **(C)** The three clusters' box plot of risk ratings was shown. ***p<0.001, *p<0.05.

The prognostic nomogram construction and evaluation

The nomogram, which consists of risk scores from the 7 m6A-related prognostic lncRNAs, and clinical risk characteristics, was employed to estimate the OS rate at 3 and 5 years. The prognostic model's risk grades demonstrated major predictive capability in the nomogram by comparison with clinical factors (figure 3A). The correlation prediction models revealed that there was a desirable consistency at 3 and 5 years between the observed rates and predicted rates in OS (figure 3B). A survival time ROC analysis was done with the survival ROC package and plotted, grouped as low risk and high risk (AUC=0.880, figure 3C). For the samples containing survival time and survival status, a survival time ROC analysis was done and plotted using the survival ROC package, grouped as metastatic stage 1/2 and stage 3/4 groups (AUC=0.688, figure 3D). The information on survival (su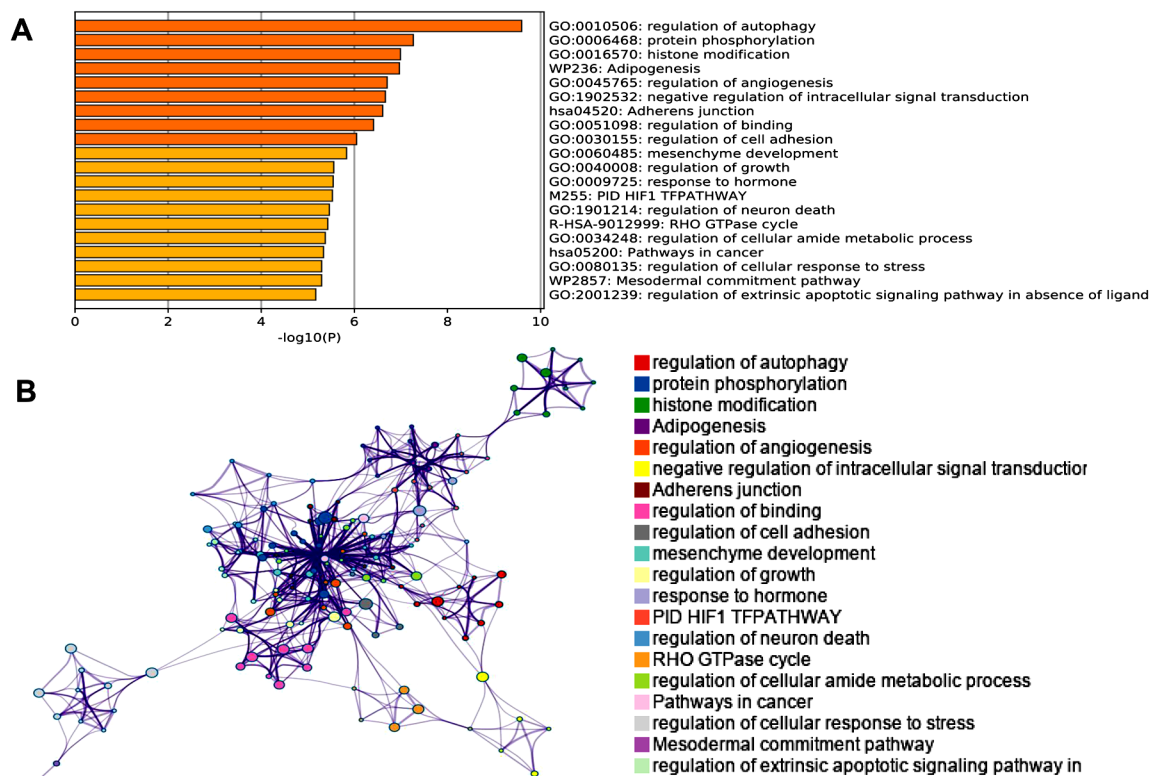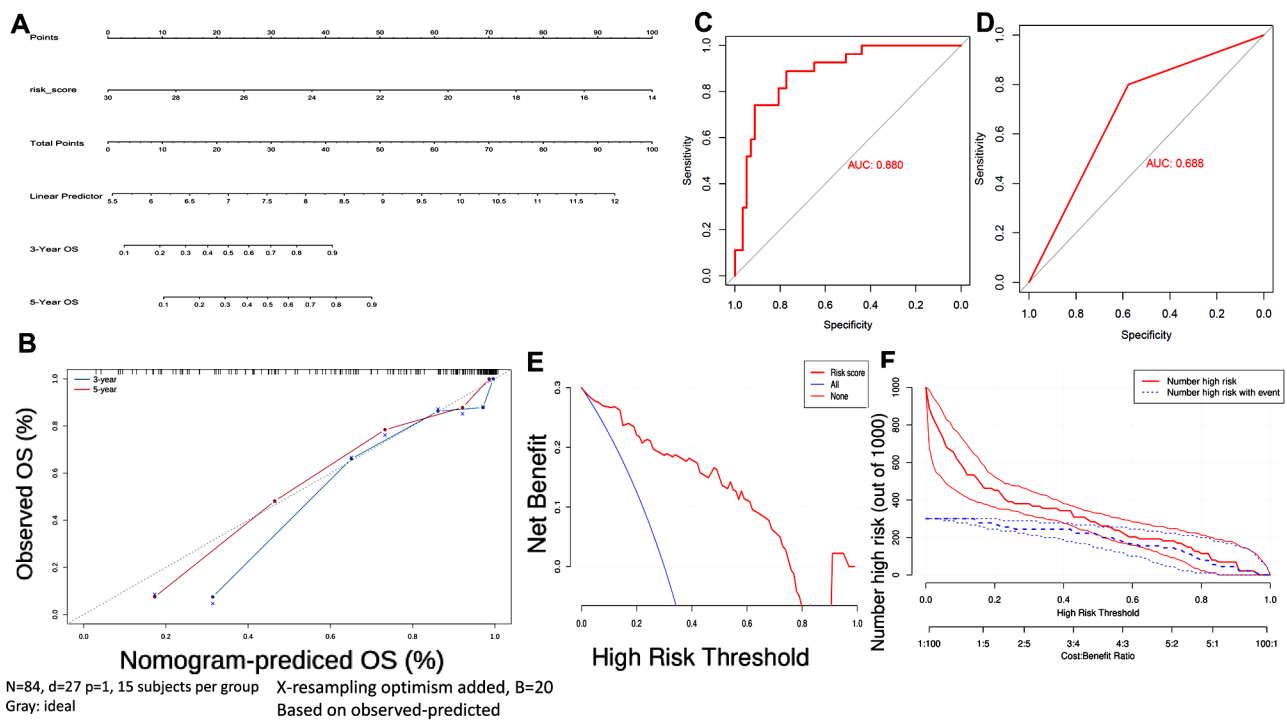rvival time and status) and the risk score were extracted and the net benefit curves were plotted using the plot decision curve function and the clinical impact curves were plotted using plot clinical impact, as shown in figure 3E and F. These data above suggested that this risk scores from the 7 m6A-related prognostic lncRNAs had the significance of predicting prognosis in OS overall survival.

The construction and functional enrichment analysis of ceRNA networks

A total of 147 lncRNA-miRNA interactional pairs were obtained using the 7 m6A-related prognostic lncRNAs in the microRNA data from mircode wibsite. Then, a total of 421 miRNA-mRNA interactional pairs were obtained using miRNA obtained above in miRWalk wibsite. Finally, a total of 278 lncRNA-miRNA-mRNA interactions were acquired by combining lncRNA-miRNA interactions with miRNA-mRNA interactions (Supplementary figure 1). The enrichment analysis was performed in two parts

in this study. The first part including 182 mRNAs from the ceRNA network were mainly enriched on regulation of autophagy, and so on (Fig. 4A, *p*.adjust < 0.05). A network plot was created using a subset of the enhanced phrases in order to more effectively depict the connections between the concepts (figure 4B).

Figure 3. The prognostic nomogram construction and evaluation. **(A)** Nomogram for estimating overall survival over three and five years using clinical data and a risk score. **(B)** Plots showing calibration for the 3- and 5-year OS nomograms. **(C)** The OS ROC of the pre-constructed nomograms was shown via the K-M curve; **(D)** The OS ROC for the groups in stages 1/2 and 3/4. **(E)** Decision curve analysis (DCA) and **(F)** The clinical impact curve of predictive nomograms.

Figure 4. Functional enrichment analysis results of mRNAs in ceRNA network. **(A)** Top 20 enriched phrases in a bar graph with p-values colored in. **(B)** The top 20 clusters are shown, colored by cluster ID, and nodes with the same cluster ID are usually located adjacent to one another.

GO and KEGG pathway analysis for 30 DEGs

The second part involving 30 DEGs were obtained in the high-risk versus low-risk comparison according to the risk score. GO and KEGG pathway enrichment analysis was carried out on 30 DEGs using the R language cluster Profiler package (*p*.adjust < 0.05), resulting in only 19 pathways in biological process (BP). The top 5 (negative regulation of protein sumoylation, regulation of ubiquitin-protein transferase activity, negative regulation of protein aceylation, regulation of protein sumoylation, positive regulation of ubiquitin-protein transferase activity) with the most significant GO functional *p*-values were shown in figure 5A-B. The BP were associated with only two genes, including MAGE (melanoma antigen gene) family member A2 (MAGEA2) and MAGEA2B (figure 5A-B, *p*.adjust < 0.05). The three pathways, including retrograde endocannabinoid signaling, gamma-aminobutyric acidergic (GABAergic) synapse and morphine addiction, were enriched by 30 DEGs on KEGG bubble diagram (figure 5C, *p*.adjust < 0.05). Furthermore, the DEGs in the high risk group were upregulated in these KEGG pathways (figure 5D, *p*.adjust < 0.05).
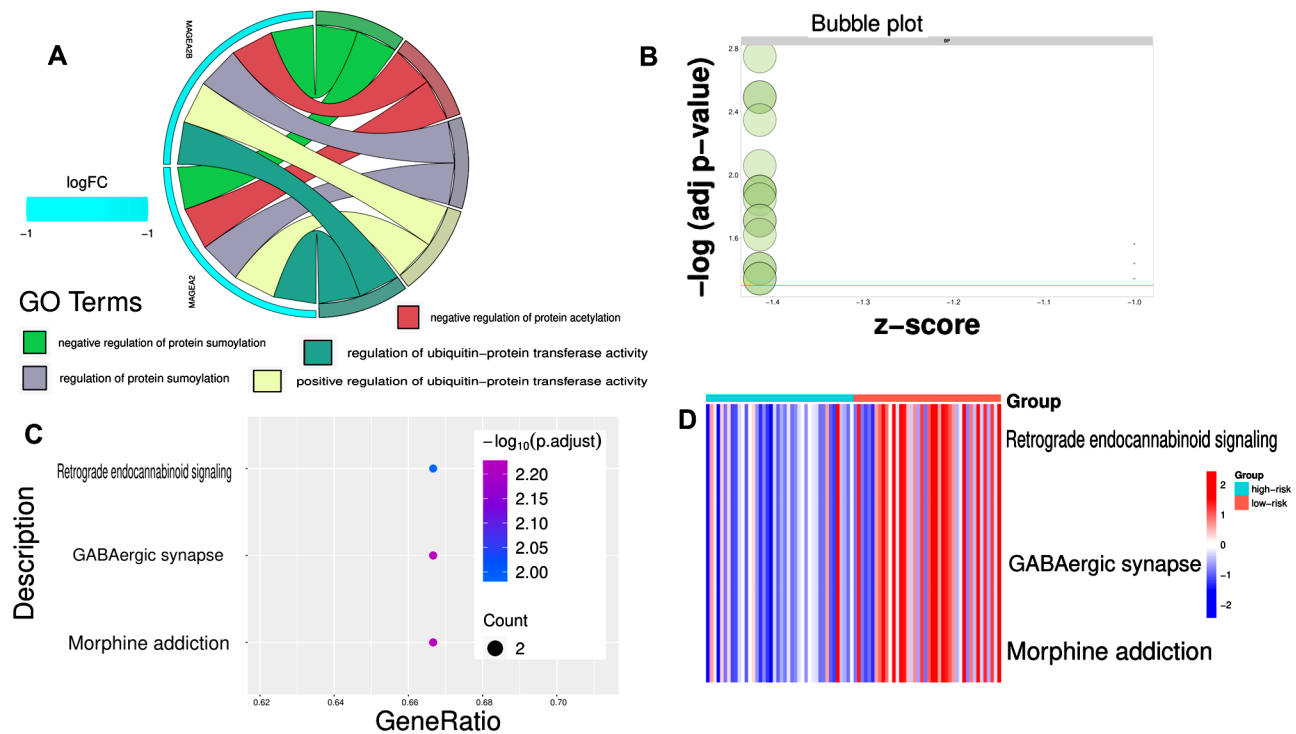

Figure 5. Enrichment analysis results of 30 DEGs. **(A-B)** Top 5 significant BP terms in GO analyses. Chord and bubble diagram. **(C-D)** KEGG analysis of enrichment. DEGs between the low-risk score group and the high-risk score group are shown in a bubble diagram and heatmap.

DISCUSSION

Our study found that the Cluster 2 from 7 m6A-related prognostic lncRNAs had the highest risk in the OS immune microenvironment. A survival time ROC analysis showed the diagnostic significance of the results between low risk and high risk (AUC=0.880), as well as between stage 1/2 and stage 3/4 groups (AUC=0.688). Many pathways were enriched by 182 mRNAs from the ceRNA network (prognostic lncRNAs-miRNA-mRNA). However, there was only 19 GO-BP enriched by 30 OS-related DEGs, and the top 5 GO-BP were associated with just two DEGs (MAGEA2 and MAGEA2B). Finally, three KEGG pathways were enriched by the 30 OS-related DEGs, including retrograde endocannabinoid signaling, GABAergic synapse, and Morphine addiction.

The tumor immune microenvironment is intricate, with tumor-infiltrating immune cells playing a pivotal role within this microenvironment [25]. The results of cancer patients may be influenced by tumor cell invasion, immunological competency, and the activation of targeted therapy and predict their response to immunotherapy [26, 27]. Immunological-related biochemical processes and the immunological microenvironment may be altered through the modulation of m6A modification or the transcription of lncRNAs [28]. In our study, there wasn't a noticeable variation in infiltrating immune cells between the low-risk and high-risk groups, which agrees with an earlier report [23], but not in line with another report [29]. The differences in these findings might be caused by different lncRNAs. However, the Cluster 2 from 7 prognostic lncRNAs had the highest risk in the OS immune microenvironment among the three clusters. Cluster 2 could be more susceptible to immunotherapy in this situation. Additionally, prognostic lncRNAs associated to m6A have been described as possible biomarkers for prognosis and immune response

prediction in patients with various cancer types [28, 30-31]. The current investigation discovered that the survival time ROC analysis in low risk and high risk groups (AUC=0.880) as well as between stage 1/2 and stage 3/4 groups (AUC=0.688) suggested that 7-lncRNA signature could serve as an independent predictor to evaluate the overall survival of OS patients. Observations have shown that LINC00538 downregulates the expression of NKD2, which promotes the development of colon cancer [32]. The LINC01982, LINC00910, LINC01474, TFPI2-DT, WWC2-AS1 and TNS1-AS1 have not been extensively covered in the literature. A recent study also showed that since immune-related lncRNAs are correlated with the tumor immunological microenvironment, they may impact the OS prognosis [15]. In line with our research, which used 26 pairings of lncRNAs,, Fu *et al.* [18] created four pairs of lncRNA prognostic characteristics to forecast osteosarcoma prognosis and showed that the immune microenvironment could be the next area of focus for OS therapy. Even Nevertheless, our lncRNA predictive characteristics are associated with m6A modulation, which sets us apart from the findings in the aforementioned papers.

Finding lncRNA's targets is an essential first step in learning more about its functions. LncRNAs are frequently involved in the ceRNA mechanism, where they act as sponges for miRNAs that control miRNA expression [33]. Numerous investigations have emphasized the critical role that lncRNA-mediated ceRNA networks in the progression of OS [34-36]. CeRNA networks enable a more thorough examination of the intricate gene relationships involved in the carcinogenic process, in addition to providing a clearer knowledge of communication between RNAs. They are also able to find new biomarkers. These 278 ceRNA networks built in our investigation could provide promising therapeutic targets, especially in the treatment of OS. Furthermore, to demonstrate the molecular function of these ceRNA networks, GO analysis was applied to analyze pathway enrichment of these mRNAs. The findings indicated that these mRNAs were mostly abundant in the control of autophagy, protein phosphorylation, histone modification, and so on. Although these biological functions are not typical of immune pathways, there are links between them and immune function. Moreover, we looked for DEGs between the low-risk and high-risk groups in an effort to shed more light on the possible molecular processes underlying the m6A-related lncRNA characteristics.

However, only 19 GO-BP were enriched by the 30 OS-related DEGs, and the top 5 GO-BP function enrichment (negative regulation of protein sumoylation, regulation of ubiqutin-protein transferase activity, negative regulation of protein aceylation, regulation of protein sumoylation, positive regulation of ubiquitin-protein transferase activity) were associated with MAGEA2 and MAGEA2B. The top 5 BP function are engaged in the control of protein modification and metabolic processes that play a significant part in immune regulation. The MAGEA2 and MAGEA2B genes are part of the MAGE sub-family of cancer-testicular antigens. In gastric signet ring cell carcinoma, MAGEA2 and MAGEA2B were identified as pivotal genes in the protein-protein interaction network, showing potential clinical value [37]. MAGEA2 also shows prognostic significance and therapeutic target in lung cancer [38]. Additionally, a research conducted by Qin *et al.* [39] shown that using immunotherapy to target MAGEA2 in order to address the paracrine control of chemoresistance is an improved approach for treating pancreatic cancer.

Besides, through KEGG enrichment analysis, only 3 KEGG pathways were enriched by the 30 OS-related DEGs, including retrograde endocannabinoid signaling, GABAergic synapse, and morphine addiction. Among these three pathways, the GABAergic synapse pathway is related to immune in the serotype A-stimulated group [40]. Moreover, the DEGs in the high risk group were upregulated in these KEGG pathways as compared to those in the low risk group. These results imply that the prognosis of OS patients may be correlated with their immunological state. Improving the clinical results of immunotherapy and removing obstacles to anticancer immune responses may be achieved by focusing on the tumor microenvironment [41, 42].

More and more m6A regulatory factors are being discovered, and here we have included only those that have been reported. Our risk model is not verified in a separate cohort since there isn't an external lncRNA expression matrix or associated clinical data. To validate the prognostic significance of the 7-lncRNA signature in predicting overall survival in OS, additional datasets and a larger range of clinical samples should be included in future research. In the future, additional confirmatory research will be conducted to address these limitations in the present study.

CONCLUSION

The present study found that m6A-associated lncRNA clusters were associated with the tumor immune microenvironment of OS. The m6A-related 7-lncRNA signature may be used to forecast an OS patient's prognosis. Moreover, the m6A-related lncRNA in ceRNA networks were related to the biological process of OS. We also found that MAGEA2 and MAGEA2B were associated with the biological processes of OS.

Abbreviations

Long noncoding RNAs (lncRNAs); osteosarcoma (OS)；Receiver Operator Characteristic (ROC); Estimation of stromal and immune cells in malignant tumour tissues using Expression data (ESTIMATE); MAGE Family Member A2 (MAGEA2); MAGE Family Member A2B (MAGEA2B); Differentially expressed genes (DEGs), reactive oxygen species (ROS), Taurine Up-Regulated 1 (TUG1); LOXL1 Antisense RNA 1 (LOXL1-AS1); Mir-100-Let-7a-2-Mir-125b-1 Cluster Host Gene (MIRI100HG); HOXD Antisense 1 (HOXD-AS1); Ewing Sarcoma Associated Transcript 1 (EWSAT1); LMCD1 Antisense RNA 1 (LMCD1-AS1)

REFERENCES

1. Siegel RL, Miller KD, Fuchs HE, Jemal A (2021) Cancer Statistics, 2021. *CA: A Cancer Journal for Clinicians. 71(1): 7-33.*
2. Harrison DJ and Schwartz CL (2017) Osteogenic sarcoma: Systemic chemotherapy options for localized disease. *Current Treatment Options in Oncology, 18(4): 24.*
3. Jafari F, Javdansirat S, Sanaie S, *et al.* (2020) Osteosarcoma: A comprehensive review of management and treatment strategies. *Annals of Diagnostic Pathology, 49: 151654.*
4. Liu J, Lian T, Chen H, *et al.* (2021) Pretreatment prediction of relapse risk in patients with osteosarcoma using radiomics nomogram based on CT: A retrospective multicenter study. *BioMed Research International, 2021: 6674471.*
5. Ferguson JL and Turner SP (2018) Bone Cancer: Diagnosis and treatment principles. *American Family Physician, 98(4): 205-13.*
6. Chen C, Xie L, Ren T, *et al.* (2021) Immunotherapy for osteosarcoma: Fundamental mechanism, rationale, and recent breakthroughs. *Cancer letters, 500: 1-10.*
7. Harrison DJ, Geller DS, Gill JD, *et al.* (2018) Current and future therapeutic approaches for osteosarcoma. *Expert Review of Anticancer Therapy, 18(1): 39-50.*
8. Tsukamoto S, Errani C, Angelini A, Mavrogenis AF (2020) Current treatment considerations for osteosarcoma metastatic at presentation. *Orthopedics, 43(5): e345-e58.*
9. Chen W, Liu S, Wang F (2021) Potential impact and mechanism of long non-coding RNAs on cancer and associated T cells. *Journal of Cancer, 12(16): 4873-82.*
10. Guo R, Zou B, Liang Y, *et al.* (2021) LncRNA RCAT1 promotes tumor progression and metastasis via miR-214-5p/E2F2 axis in renal cell carcinoma. *Cell Death & Disease, 12(7): 689.*
11. Che D, Fang Z, Mai H, *et al.* (2021) The lncRNA ANRIL gene rs2151280 GG genotype is associated with increased susceptibility to recurrent miscarriage in a Southern Chinese population. *J Inflammation Research, 14: 2865-72.*
12. Liu X, Yin Z, Xu L, *et al.* (2021) Upregulation of LINC01426 promotes the progression and stemness in lung adenocarcinoma by enhancing the level of SHH protein to activate the hedgehog pathway. *Cell Death & Disease, 12(2): 173.*
13. Hou T, Ye L, Wu S (2021) Knockdown of LINC00504 Inhibits the Proliferation and Invasion of Breast Cancer via the Downregulation of miR-140-5p. *OncoTargets and Therapy, 14: 3991-4003.*
14. Chen K, Zhang Z, Yu A, *et al.* (2020) lncRNA DLGAP1-AS2 knockdown inhibits hepatocellular carcinoma cell migration and invasion by regulating miR-154-5p methylation. *BioMed Research International, 2020: 6575724.*
15. Huang Q, Lin Y, Chen C, *et al.* (2021) Immune-related LncRNAs affect the prognosis of osteosarcoma, which are related to the tumor immune microenvironment. *Frontiers in Cell and Developmental Biology, 9: 731311.*
16. Yang M, Zheng H, Xu K, *et al.* (2022) A novel signature to guide osteosarcoma prognosis and immune microenvironment: Cuproptosis-related lncRNA. *Frontiers in Immunology, 13: 919231.*
17. Zhang J, Huang C, Zhu G, *et al.* (2022) Selection of lncRNAs that influence the prognosis of osteosarcoma based on copy number variation data. *Journal of Oncology, 2022: 8024979.*
18. Fu R and Hong X (2022) Discovery of new therapeutic targets for osteosarcoma treatment based on immune-related lncRNAs in the tumor microenvironment. *BioMed Res Int, 2022: 3113857.*
19. Xie H, Shi M, Liu Y, *et al.* (2022) Identification of m6A- and ferroptosis-related lncRNA signature for predicting immune efficacy in hepatocellular carcinoma. *Frontiers in Immunology, 13: 914977.*
20. Feng ZH, Liang YP, Cen JJ, *et al.* (2022) m6A-immune-related lncRNA prognostic signature for predicting immune landscape and prognosis of bladder cancer. *J Translational Medicine, 20(1): 492.*
21. Hou P, Meng S, Li M, *et al.* (2021) LINC00460/DHX9/IGF2BP2 complex promotes colorectal cancer proliferation and metastasis by mediating HMGA1 mRNA stability depending on m6A modification. *J Experimental & Clinical Cancer Research, 40(1): 52.*
22. Lang C, Yin C, Lin K, *et al.* (2021) A modification of lncRNA PCAT6 promotes bone metastasis in prostate cancer through IGF2BP2-mediated IGF1R mRNA stabilization. *Clinical and Translational Medicine, 11(6): e426.*
23. Bi Y, Meng D, Wan M, *et al.* (2022) m6A-related lncRNAs predict overall survival of patients and regulate the tumor immune microenvironment in osteosarcoma. *Computational Intelligence and Neuroscience, 2022: 9315283.*
24. Pan J, Huang Z, Xu Y (2021) m5C-related lncRNAs predict overall survival of patients and regulate the tumor immune microenvironment in lung adenocarcinoma. *Frontiers in Cell and Developmental Biology, 9: 671821.*
25. Hayase E and Jenq RR (2021) Role of the intestinal microbiome and microbial-derived metabolites in immune checkpoint blockade immunotherapy of cancer. *Genome Medicine, 13(1): 107.*
26. Price G, Bouras A, Hambardzumyan D, Hadjipanayis CG (2021) Current knowledge on the immune microenvironment and emerging immunotherapies in diffuse midline glioma. EBioMedicine. 2021;69:103453.
27. Zhang K, Ping L, Du T, *et al.* (2021) A ferroptosis-related lncRNAs signature predicts prognosis and immune microenvironment for breast cancer. *Frontiers in Molecular Biosciences, 8: 678877.*

28. Xu F, Huang X, Li Y, *et al.* (2021) m(6)A-related lncRNAs are potential biomarkers for predicting prognoses and immune responses in patients with LUAD. *Molecular Therapy Nucleic acids,* **24**: 780-91.

29. Zheng D, Yu L, Wei Z, *et al.* (2021) N6-methyladenosine-related lncRNAs are potential prognostic biomarkers and correlated with tumor immune microenvironment in osteosarcoma. *Frontiers in Genetics,* **12**: 805607.

30. Zhong F, Yao F, Cheng Y, *et al.* (2022) m6A-related lncRNAs predict prognosis and indicate immune microenvironment in acute myeloid leukemia. *Scientific Reports,* **12(1):** 1759.

31. Wang Y, Zhu GQ, Tian D, *et al.* (2022) Comprehensive analysis of tumor immune microenvironment and prognosis of m6A-related lncRNAs in gastric cancer. *BMC Cancer,* **22(1):** 316.

32. Tang H, Dou Y, Meng Y, (2020) LINC00538 promotes the progression of colon cancer through inhibiting NKD2 expression. *J BUON: Official Journal of the Balkan Union of Oncology,* **25(6):** 2657-64.

33. Guo K, Qian K, Shi Y, *et al.* (2021) LncRNA-MIAT promotes thyroid cancer progression and function as ceRNA to target EZH2 by sponging miR-150-5p. *Cell Death & Disease,* **12(12):** 1097.

34. Lin C, Miao J, He J, *et al.* (2022) The regulatory mechanism of LncRNA-mediated ceRNA network in osteosarcoma. *Scientific Reports,* **12(1):** 8756.

35. Xiao X, Jiang G, Zhang S, *et al.* (2021) LncRNA SNHG16 contributes to osteosarcoma progression by acting as a ceRNA of miR-1285-3p. *BMC Cancer,* **21(1):** 355.

36. Wan D, Qu Y, Zhang L, *et al.* (2020) The lncRNA LINC00691functions as a ceRNA for miRNA-1256 to suppress osteosarcoma by regulating the expression of ST5. *OncoTargets and Therapy,* **13**: 13171-81.

37. Zhao ZT, Li Y, Yuan HY, *et al.* (2020) Identification of key genes and pathways in gastric signet ring cell carcinoma based on transcriptome analysis. *World Journal of Clinical Cases,* **8(4):** 658-69.

38. Ujiie H, Kato T, Lee D, *et al.* (2017) Overexpression of MAGEA2 has a prognostic significance and is a potential therapeutic target for patients with lung cancer. *Int J Oncology,* **50(6):** 2154-70.

39. Qin H, Chen J, Bouchekioua-Bouzaghou K, *et al.* (2023) Immunization with a multi-antigen targeted DNA vaccine eliminates chemoresistant pancreatic cancer by disrupting tumor-stromal cell crosstalk. *Journal of Translational Medicine,* **21(1):** 702.

40. An Q, Chen S, Zhang L, *et al.* (2022) The mRNA and miRNA profiles of goat bronchial epithelial cells stimulated by Pasteurella multocida strains of serotype A and D. *PeerJ,* **10**: e13047.

41. Lei Y, Junxin C, Yongcan H, *et al.* (2020) Role of microRNAs in the crosstalk between osteosarcoma cells and the tumour microenvironment. *Journal of Bone Oncology,* **25**: 100322.